



Science Arts & Métiers (SAM)

is an open access repository that collects the work of Arts et Métiers Institute of Technology researchers and makes it freely available over the web where possible.

This is an author-deposited version published in: <https://sam.ensam.eu>
Handle ID: <http://hdl.handle.net/10985/7543>

To cite this version :

Daniel KERMER, Guillaume FROMENTIN, Olivier LOUTAN, Kossi AGEBEBIADE, Jacques GIOVANOLA - Micro-orthogonal Cutting of Metals - In: Precision Engineering and Nanotechnology International Conference, Switzerland, 2008-05-18 - Proceedings of the European Society for Precision Engineering and Nanotechnology International Conference - 2008

Any correspondence concerning this service should be sent to the repository

Administrator : scienceouverte@ensam.eu



Micro-orthogonal Cutting of Metals

D., Kremer¹, G. Fromentin², O. Loutan¹, K. Agbebiade¹, J. Giovanola¹

¹*Ecole Polytechnique Fédérale de Lausanne, Switzerland,*

²*Arts et Metiers ParisTech, LaBoMaP, Rue Porte de Paris, 71250 CLUNY*

jacques.giovanola@epfl.ch

Abstract

Industrial application of micro-milling faces several scientific, technological and economic issues. To address these issues, we have developed a micro-orthogonal cutting facility in which chip thickness can be controlled to within a micron and cutting forces can be measured. This paper presents the facility and preliminary results of micro-orthogonal cutting on copper, in the form of span observations, cutting ratio measurements and estimates of shear angles and cutting forces.

1 Introduction

Micro-cutting and in particular micro-milling of ductile metals and more brittle materials has attracted significant attention for its range of potential practical applications in manufacturing of high technology, miniaturized products [1]. Its more wide-spread application hinges upon resolving several scientific, technological and economic issues. Economic and technological issues include the lack of 1) high speed high precision spindles with suitable tool spanning systems capable of achieving high speed cutting conditions and permitting an economical material removing rate, 2) tools with appropriate cutting edge quality and properties, and 3) well documented application databases to select tool geometry and cutting conditions for specific materials. Scientific issues involve among other questions 1) the understanding of the role of characteristic material microstructural dimensions and of cutting edge radius on the cutting size effect and 2) the integration of material damage and separation processes in models of metal cutting.

To address these issues, we are implementing an integrated approach covering from micro-modelling of fracture under predominantly shear loading to developing high speed, high precision spindles. In this paper, we present preliminary results of a basic

investigation of micro-orthogonal cutting of metal aiming at 1) understanding and modelling micro-cutting processes, 2) identifying size effects by comparison with macro-cutting results and 3) assessing the transferability of macro-cutting data to micro-cutting.

2 Micro-orthogonal cutting facility.

Figure 1 shows the micro-orthogonal cutting facility (a), the specimen (b), and the cutting tool (c). The X-axis consists of a hydrostatic linear guideway with a electrical linear motor. The detailed kinematic, static and dynamic characterizations of the system are still underway. Available results can be summarized as follows. The transverse stiffness of the X-axis is greater than $250 \text{ N}/\mu\text{m}$ for a supply pressure of 10 bars. The stroke is 100 mm with a maximum speed of around 1.2 m/s (over 20 mm) with peak accelerations of approximately 3g. Estimates and measurements indicate maximum dynamic yaw and tilt displacements at the table edges on the order of $\pm 3 \mu\text{m}$ for an acceleration of 3 g and a supply pressure of 10 bars. A piezo-actuator controls the Z-axis position ($\pm 250 \text{ nm}$) and the depth of cut by means of an Eddy current sensor and a feedback control loop. Currently the control of the span thickness is better than $\pm 1 \mu\text{m}$, all error sources included. The Z-axis also provides a measurement of the Z cutting force through the control voltage of the piezo actuator or a separate force sensor. Another sensor, built, but not tested, will measure X cutting forces.

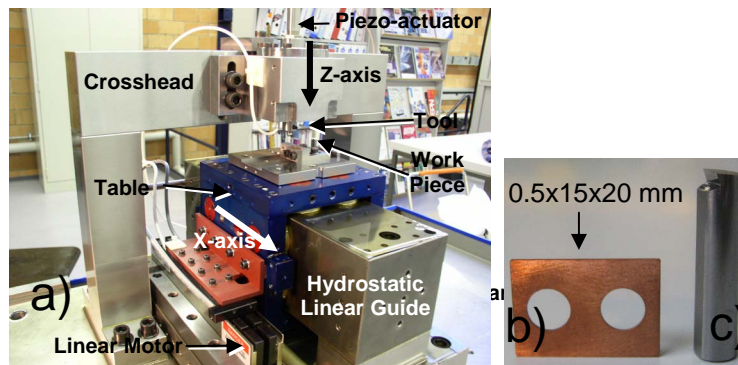


Figure 1 a) Micro-orthogonal cutting facility b) specimen c) WC tool

3 Results of preliminary orthogonal cutting experiments.

We performed orthogonal cutting experiments on copper specimens with the facility of Figure 1, varying depth of cut h_c (5 and 10 μm), rake angle γ (20° , 0° , -20°) and cutting speed v_c (440, 660, 880 mm/s). For these experiments, we characterized the morphology and dimensions of the span and the roughness of the specimen surface; we determined the cutting ratio and estimated the cutting forces. In separate experiments we also performed proof-of-concept measurements of the Z thrust force and photographed the formation of the span. Figures 2 to 4 and Tables 1 and 2 illustrate the results of these experiments.

Table 1: Roughness R_a and cutting depth accuracy as a function of cutting parameters

| Cutting depth 5 μm | | | | Cutting depth 10 μm | | | |
|--------------------------------|------|------|------|--------------------------------|------|------|------|
| Rake angle | 20° | | | Rake angle | 20° | | |
| Cutting speed, mm/s | 880 | 660 | 440 | Cutting speed, mm/s | 880 | 660 | 440 |
| R_a , μm | 0.66 | 0.57 | 0.47 | R_a , μm | 0.51 | 0.42 | 0.57 |
| Error on h_c , μm | -0.1 | 0.1 | -0.3 | Error on h_c , μm | -1.0 | 0.2 | -0.9 |
| Rake angle | 0° | | | Rake angle | 0° | | |
| Cutting speed, mm/s | 880 | 660 | 440 | Cutting speed, mm/s | 880 | 660 | 440 |
| R_a , μm | 0.72 | 0.78 | 0.58 | R_a , μm | 0.39 | 0.46 | 0.59 |
| Error on h_c , μm | -0.7 | -0.6 | -1.0 | Error on h_c , μm | 0.2 | 0.0 | 0.3 |
| Rake angle | -20° | | | Rake angle | -20° | | |
| Cutting speed, mm/s | 880 | 660 | 440 | Cutting speed, mm/s | 880 | 660 | 440 |
| R_a , μm | 0.94 | 0.49 | 0.60 | R_a , μm | 0.68 | 0.55 | 0.55 |
| Error on h_c , μm | -0.8 | -0.8 | -0.3 | Error on h_c , μm | 0.6 | 0.9 | 0.1 |

The thickness of material removed h_c varies at most by 1 μm , independently of the cutting parameters investigated, showing that we have a good control of the depth of cut. The resulting roughness of the specimen surface does not follow any clear trend with varying cutting parameters and ranges between 0.39 and 0.94 (Table 1). Micro-spans look rather similar to their macroscopic counterparts, except for their small size. Spans produced by a tool with $\gamma = 20^\circ$ are strongly curled up whereas spans associated with the other 2 rake angles are almost flat (Figures 2 and 3). The thickness of the cut span h_s can vary by several μm along its length (Figure 2b). The reason for this variation is not known yet.

Spans vary in width too (Figure 3a). Whereas the surface sliding on the rake face is rather smooth – showing only the grooving pattern caused by the roughness of the

rake face – the free surface is strongly serrated with the size and the spacing of the serrations varying along the span length, and also as a function of cutting parameters (Figure 3a). The serrations or folds are more pronounced for a negative rake angle and their structure changes with cutting speed (Figure 3b).

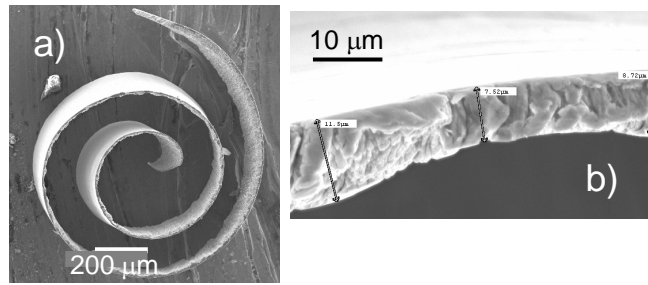


Figure 2 SEM photographs of a copper span a) overall view, b) edge view showing thickness variations ($h_c < 5 \mu\text{m}$, $\gamma = 20^\circ$).

The cutting ratios R_c estimated on the basis of the depth of cut and span thickness measurements range from about 0.08 to 0.13 for $\gamma = -20^\circ$ and 0° , and 0.19 to 0.22 for $\gamma = 20^\circ$. The cutting ratio is not very sensitive to v_c (Figure 4).

Using the measured cutting ratios and the Lee and Shaffer model [2], one can

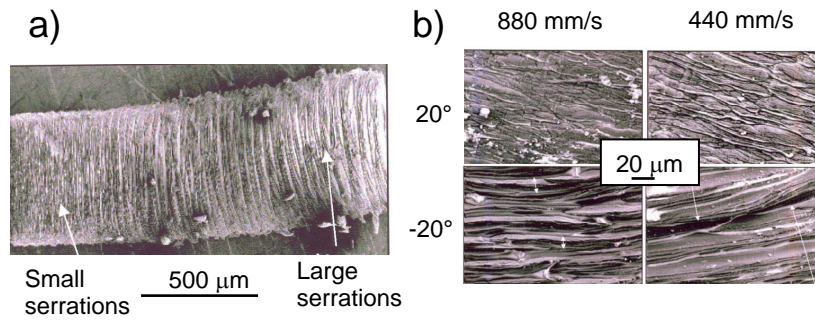


Figure 3 Span appearance a) overall view ($h_c = 10 \mu\text{m}$, $v_c = 440 \text{ mm/s}$, $\gamma = -20^\circ$); b) fold appearance on span surface as a function of v_c and γ .

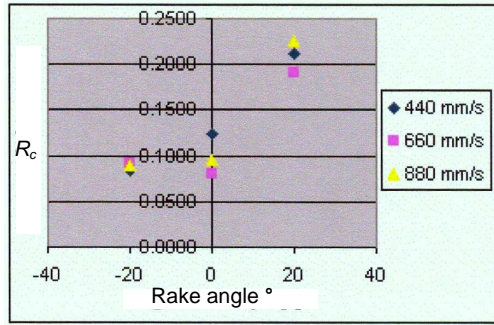


Figure 4 Cutting ratio as a function of v_c and γ ($h_c=10 \mu\text{m}$).

estimate shear angles and cutting forces. With a flow strength of 270 MPa for copper and $h_c=10 \mu\text{m}$, we obtain the data in Table 2. Preliminary direct measurements of the Z-axis repelling force for $\gamma=20^\circ$ and $h_c=10 \mu\text{m}$ give values in the range 4 to 6 N.

Table 2: estimates of cutting parameters ($h_c=10 \mu\text{m}$)

| Rake angle γ [°] | 20 | 0 | -20 |
|-------------------------|-------------|-------------|-------------|
| Cutting ratio R_c | 0.19 – 0.22 | 0.08 – 0.13 | 0.08 – 0.09 |
| Shear angle ϕ [°] | 10.8 – 12.6 | 4.5 – 7.4 | 4.2 – 4.7 |
| X-force [N] | 8.4 – 7.4 | 18.2 – 11.7 | 19.8 – 17.8 |
| Z-force [N] | 5.7 – 4.7 | 15.5 – 9.0 | 17.1 – 15.1 |

4 Summary and perspectives

An experimental platform for investigating micro-cutting has been developed and its performances have been partially validated. Encouraging preliminary cutting data have been obtained for copper. Work continues to characterize fully dynamic behaviour and precision of the facility, and to integrate reliable sensors for measuring cutting forces. Additional work will focus on developing cutting tools with sharper and more regular cutting edges and on demonstrating the importance of material separation processes in controlling cutting forces.

References:

- [1] Masuzawa, T., “State of the Art of Micromachining” *Annals of CIRP*, **49**, 2, (2000), p. 473.
- [2] Oxley, P.L.B., *The Mechanics of Machining*, Ellis Horwood, Chichester, (1989).